Available online at www.sciencedirect.com
ScienceDirect
Trans. Nonferrous Met. Soc. China 20(2010) 1463−1469
Transactions of Nonferrous Metals Society of China
www.tnmsc.cn

Preparation and characterization of CuO-CoO-MnO/SiO_2 nanocomposite aerogels as catalyst carriers

ZHAO Yue-qing(赵越卿)[1, 2], ZHAO Hai-lei(赵海雷)[2], LIANG Ying-hua(梁英华)[3], JIA Qian-yi(贾千一)[4], ZHANG Bo-bo(张波波)[3]

1. College of Light Industry, Hebei Polytechnic University, Tangshan 063000, China;
2. College of Materials Science and Engineering, University of Science and Technology Beijing, Beijing 100083, China;
3. College of Chemical Engineering, Hebei Polytechnic University, Tangshan 063009, China;
4. College of Materials Science and Engineering, Hebei Polytechnic University, Tangshan 063009, China

Received 20 November 2009; accepted 22 March 2010

Abstract: CuO-CoO-MnO/SiO_2 nanocomposite aerogels were prepared by using tetraethyl orthosilicate (TEOS) as Si source, and aqueous solution of Cu, Co and Mn acetates as the precursors via sol-gel process and ethanol supercritical drying technique. The gelatination mechanism was investigated by nuclear magnetic resonance (NMR) and X-ray photoelectron spectroscopy (XPS). The microstructure and composition of the CuO-CoO-MnO/SiO_2 nanocomposite aerogels were characterized by field emission scanning electron microscopy (FE-SEM), transmission electron microscopy (TEM), electron dispersive spectroscopy (EDS) and XPS. The specific surface area, pore size and pore size distribution of the nanocomposite aerogels were determined by the Brunauer–Emmett–Teller (BET) method. The products were analyzed by gas chromatography (GC). The results show that the CuO-CoO-MnO/SiO_2 nanocomposite aerogels are porous, with a particle size distribution of 10–150 nm, a pore size distribution of 2–16 nm, an average pore size of 7.68 nm, and a specific surface area of 664.4−695.8 m^2/g. The molar fraction of transition metals in the nanocomposite aerogels is 0.71%−13.77%. This kind of structure is favorable not only to increase the loading of catalysts, but also to make full use of the effect of transition metal oxides as cocatalysts; CuO-CoO-MnO/SiO_2 nanocomposite aerogels can be used as a novel catalyst carrier in the safer and environment-friendly synthesis of diphenyl carbonate and other fields of catalysis.
Key words: nanocomposite aerogel; preparation; characterization; catalyst carrier

1 Introduction

Porous materials have tremendous importance in materials science and engineering, mainly due to their high specific surface area and variable porosity. These features are important for heterogeneous catalysis, gas sensing and separation science[1−5]. Aerogels are nanoporous materials. Unique structural and morphological properties, including high inner specific surface area, open porosity, large pore volume, and excellent temperature stability, render aerogels promising materials for catalytic applications[6]. Altering the chemical composition of aerogel framework to generate catalytically selective high specific surface area materials is an area of current topical heterogeneous catalysis as both catalysts and catalyst carriers[7]. Composite aerogels permit the combination of redox components and structural components to further tailor the properties of heterogeneous catalysts[8−9]. CuO-CoO-MnO/SiO_2 nanocomposite aerogels can be used as a novel catalyst carrier in the synthesis of diphenyl carbonate (DPC), and the yield of DPC reaches up to 27.14% (mass fraction).

DPC is the precursor of polycarbonate (PC). PC has been recognized as the attractive engineering thermoplastics, which is widely used in industries as substitutes for metals and glasses because of its impact strength, heat resistance and transparency[7]. There is increasing demand for a safer and environmentally favorable process for DPC production. In recent years, some porous carriers, such as active carbon, molecular sieve, porous alumina and the like, have been used in the synthesis of DPC, however, the yield of DPC is less than 6.2%. This is considered to be due to lack of active transition metals and transition metal oxides in the

Foundation item: Project(10215606D) supported by the Science and Technology Development Foundation of Hebei province, China
Corresponding author: ZHAO Yue-qing; Tel: +86-315-2797086; E-mail: zhaoyueqing123@163.com
DOI: 10.1016/S1003-6326(09)60322-8

structure[7].

Due to the high porosity and specific surface area of plain SiO_2 aerogel, the incorporation of cocatalysts CuO, CoO and MnO with SiO_2 aerogel may have the possibility to increase the specific surface area of cocatalysts. Accordingly, CuO-CoO-MnO/SiO_2 nanocomposite aerogels were prepared via sol-gel process. The microstructure characteristics of the nanocomposite aerogels were investigated.

2 Experimental

2.1 Preparation of CuO-CoO-MnO/SiO_2 nanocomposite aerogels

Tetraethyl orthosilicate (TEOS) (Tianjin Beifang Tianyi Chemical Reagent Factory, China), $Cu(OAc)_2$, $Mn(OAc)_2$, $Co(OAc)_2$ (Tianjin Guangfu Institute of Fine Chemical Industry, China), ethanol, HCl, and aqua ammonia (Tangshan Lubei District Chemical Plant, China) were used as raw materials. $Cu(OAc)_2$, $Co(OAc)_2$ and $Mn(OAc)_2$ were dissolved with distilled water, and the starting solutions of $Cu(OAc)_2$, $Co(OAc)_2$ and $Mn(OAc)_2$ were mixed with the mole ratio of 1:1:1. Homogeneous silica sol was prepared by mixing TEOS, H_2O and ethanol with the mole ratio of 1:4:8 in 100 mL polyethylene vials at 50 °C for 0.5 h. The aqueous solution of Cu, Co and Mn acetates and silica sol were combined with the mole ratio of 1:4−1:2, stirred for 40 min, and the pH value was adjusted to 3.0 by dropwise addition of hydrochloric acid with concentration of 1.2 mol/L. Composite wet gels were obtained in base catalyzed system by dropwise addition of 2.5 mol/L aqua ammonia, and the pH value was 4.0. The wet gels were exchanged with ethanol two times and then aged in ethanol solvent for 3 d to increase gel firmness. The gels exchanged with ethanol were dried under hot supercritical conditions by raising the drier temperature to 243 °C, pressure 6.5 MPa and maintaining the conditions for 3 h, followed by venting of ethanol gas over 120 min to obtain nanocomposite aerogels. The composite aerogels were placed in a furnace and heat-treated at 500 °C in air for 3 h to produce CuO-CoO-MnO/SiO_2 nanocomposite aerogels.

2.2 Analysis and characterization techniques

The gelatination mechanism of CuO-CoO-MnO/SiO_2 composite sols was examined by ^{29}Si nuclear magnetic resonance (^{29}Si NMR, INFINITY PLUS 300WB, Varian Company, USA) and X-ray photoelectron spectroscopy (PHI1600 ESCA, PerkinElmer Company, USA). The microstructure and composition of the nanocomposite aerogels were characterized by field emission scanning electron microscopy (S-4500, Hitachi Company, Japan), transmission electron microscopy (JEM-2010, Japanese Electronic Company, Japan) and electron dispersive spectrum analysis (VANTAGE 4.0, Noran Company, USA), respectively. The specific surface area, pore size and pore size distribution of the nanocomposite aerogels were determined by the Brunauer–Emmett–Teller method (AUTOSORB-1, Quantachrome Instruments, USA).

3 Results and discussion

3.1 Gelatination mechanism of nanocomposite aerogels

Silicon-29 is the only magnetic isotope of the three naturally occurring isotopes (i.e., ^{28}Si, ^{29}Si and ^{30}Si), and the chemical shifts of most silicon compounds fall between 50×10^{-6} and -200×10^{-6}. Solid state ^{29}Si NMR has been successfully applied to a wide range of crystalline and amorphous silicates or other related materials[10]. There are five types of $Si(O_{1/2})_4$ tetrahedral units designated as Q^0, Q^1, Q^2, Q^3 and Q^4 that can be present in the ^{29}Si NMR spectra (Q^n: Q corresponds to silicone atoms bonded to four oxygen atoms, while *n* that varies between 1 and 4 is the number of silicone atoms bonded to these oxygen atoms), Q^0 is designated a single tetrahedron, Q^1 is an end group, Q^2 is a middle group, Q^3 is a branching site, and Q^4 is a cross-linking group[10−12]. Fig.1 shows the stereo-chemical structure of each Q^n unit in plain SiO_2 aerogels.

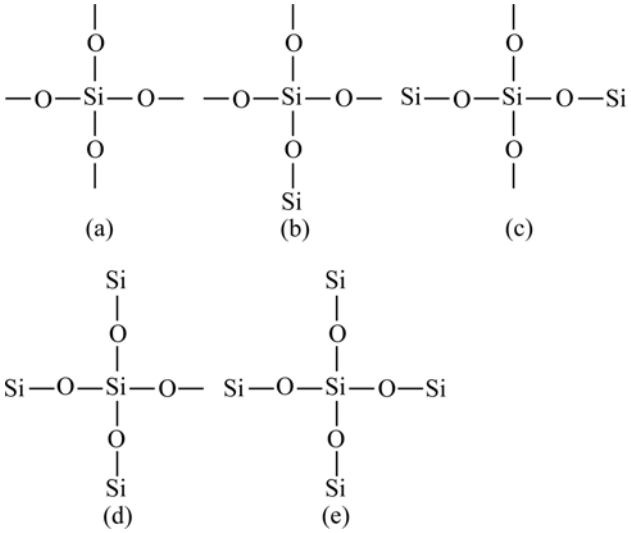

Fig.1 Stereo-chemical structure representations of five tetrahedral Q^n units in plain SiO_2 aerogels: (a) Q^0; (b) Q^1; (c) Q^2; (d) Q^3; (e) Q^4

Figs.2 (a) and (b) show the ^{29}Si MAS NMR spectra of SiO_2 aerogel heat-treated at 500 °C and the ^{29}Si MAS NMR spectra of CuO-CoO-MnO/SiO_2 nanocomposite aerogel heat-treated at 500 °C, respectively, as well as

the sub-units Q^0, Q^1, Q^2, Q^3 and Q^4. From Fig.2(a), it can be seen that Q^0, Q^1, Q^2, Q^3 and Q^4 indicate Q^0—Si (i.e. $Si(OX)_4$, X═H or CH_3), Q^1—Si (i.e. $Si(OSi\equiv)(OX)_3$), Q^2 — Si (i.e. $Si(OSi\equiv)_2(OX)_2$), Q^3 — Si (i.e. $Si(OSi\equiv)_3(OX)$) and Q^4 — Si (i.e. $Si(OSi\equiv)_4$), respectively[13]. The peak at -110×10^{-6} (Q^3) indicates the dominant component, and then peaks at -114×10^{-6} (Q^4) and -106×10^{-6} (Q^2) in the spectra of silica aerogel heat-treated at 500 °C.

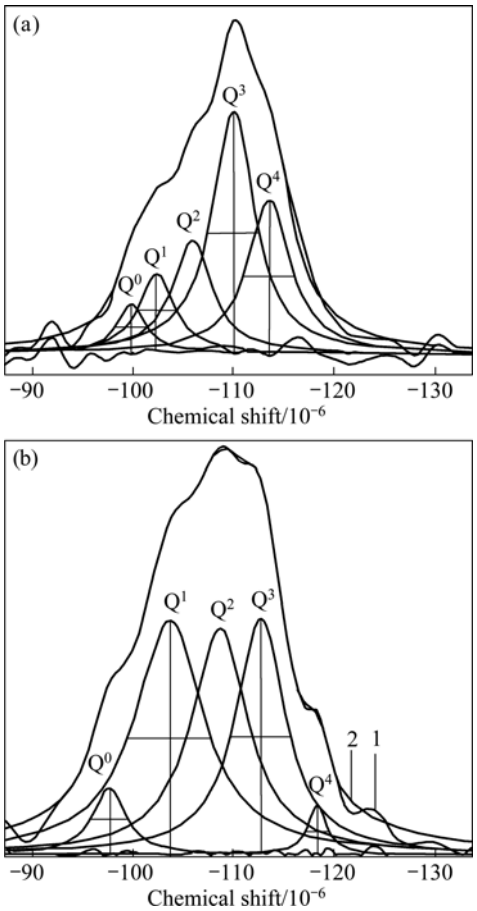

Fig.2 ^{29}Si MAS NMR spectra of silica aerogel (a) and CuO-CoO-MnO/SiO_2 nanocomposite aerogel (b) heat-treated at 500 °C as well as their sub-units Q^0, Q^1, Q^2, Q^3 and Q^4

From Fig.2(b), it can be seen that the curve 1 indicates the experimental spectrum obtained by ^{29}Si NMR. Q^0, Q^1, Q^2, Q^3 and Q^4 indicate the deconvolution of the original spectra, and the smooth curve 2 indicates a simulated spectrum by the addition of the integrated peaks Q^0, Q^1, Q^2, Q^3 and Q^4. As we can see from Fig.2(b), curves 1 and 2 almost coincide each other. The chemical shifts of the peaks Q^0, Q^1, Q^2, Q^3 and Q^4 fall between -96×10^{-6} and -118×10^{-6} in the spectra of nanocomposite aerogel heat-treated at 500 °C. Peaks at -96×10^{-6}, -103×10^{-6}, -108×10^{-6}, -112×10^{-6} and -118×10^{-6} indicate Q^0—Si (i.e. $Si(OM)_4$, M═Cu, Co, Mn, or H and CH_3), Q^1—Si (i.e. $Si(OSi\equiv)(OM)_3$), Q^2—Si (i.e. $Si(OSi\equiv)_2(OM)_2$), Q^3—Si (i.e. $Si(OSi\equiv)_3(OM)$) and Q^4—Si (i.e. $Si(OSi\equiv)_4$), respectively. From Fig.2(b), it can be seen that Q^0, Q^1, Q^2, Q^3 and Q^4 $Si(O_{1/2})_4$ tetrahedral sub-units exist in the nanocomposite aerogel processed under supercritical ethanol conditions after calcination at 500 °C, and Q^1, Q^2 and Q^3 sub-units are the dominant components in the structure. The relative percents of Q^n sub-units are obtained by determining the area under the five Q^n peaks. The chemical shift values and relative percents of Q^n sub-units in samples of CuO-CoO-MnO/SiO_2 nanocomposite aerogel and silica aerogel heat-treated at 500 °C are listed in Table 1.

Compared with the spectrum in Fig.2(b) and the five sub-units of CuO-CoO-MnO/SiO_2 nanocomposite aerogel with the spectrum in Fig.2(a) and the sub-units of SiO_2 aerogel in Fig.2 and Table 1, the relative percents of Q^4 and Q^3 obviously decrease from 26.43% and 40.93% to 2.33% and 26.94%, respectively. However, the relative percents of Q^1 and Q^2 increase from 10.38% and 17.12% to 36.55% and 29.25%, respectively. It appears that for CuO-CoO-MnO/SiO_2 nanocomposite aerogel heat-treated at 500 °C, most of the Si atoms participate in the three-dimensional gel network, with 36.55% as Q^1 end groups, 29.25% as Q^2 middle groups in a linear fashion and 26.94% as Q^3 branching sites. Only 2.33% of the Si atoms participate in the network in cross-linking groups, and 4.88% of the Si atoms participate in the terminal Si sites or free $Si(OM)_4$. This indicates that most of the active transition metals as cocatalysts are present in surface groups in the nanocomposite aerogel, and this structure is favourable to catalysis of the active transition metals in catalystic reaction.

Compared with the sample of silica aerogel, the chemical shift values of the five sub-units exhibit some shifts in Fig.2(b) and Table 1, these spectral features are probably caused by the formation of metal binding sites[10,13−14]. The lines broadening is associated with

Table 1 Chemical shift values (δ) and relative percents of Q^n sub-units in samples of SiO_2 aerogel and CuO-CoO-MnO/SiO_2 nanocomposite aerogel heat-treated at 500 °C

Sample	Q^0		Q^1		Q^2		Q^3		Q^4	
	$\delta/10^{-6}$	Relative percent/%	$\delta/10^{-6}$	Relative percent/%	$\delta/10^{-6}$	Relative percent/%	$\delta/10^{-6}$	Relative percent/%	$\delta/10^{-6}$	Relative percent/%
SiO_2 aerogel	−100	5.20	−102	10.38	−106	17.12	−110	40.93	−114	26.43
Nanocomposite aerogel	−96	4.88	−103	36.55	−108	29.25	−112	26.94	−118	2.33

the presence of bridging effect of oxygen and transition metals (i.e. —O—M—O—, M=Cu, Co or Mn) in the three dimensional network of CuO-CoO-MnO/SiO_2 nanocomposite aerogel, and the broadened spectra with similar line shapes indicate that the original sub-units structures are still present.

$(EtO)_3Si—O—M—O—Si(OEt)_3$ was formed by using TEOS (i.e. $Si(OEt)_4$) and acetates of Cu, Co and Mn via sol-gel process under the catalysis of catalysts. Wet gels with one to three-dimensional structure were obtained by the proportion variations of TEOS and acetates of transition metals. The basic reaction equation is shown as follows[8, 15]:

$$M^{2+}+2Si(OEt)_4 \longrightarrow (EtO)_3Si—O—M—O—Si(OEt)_3 \quad (1)$$

3.2 Composition and structure characteristics of nanocomposite aerogels

Fig.3 shows the XPS spectra and the molar fractions of atoms in CuO-CoO-MnO/SiO_2 nanocomposite aerogel heat-treated at 500 °C, and the original molar fraction of CuO, CoO and MnO in precursors of the composite sol is 50%. From Fig.3, it can be seen that the molar fractions of Cu, Co and Mn are 3.0%, 1.3% and 3.6%, respectively, in the nanocomposite aerogel after solvent exchange with ethanol two times and CO_2 supercritical drying process. Compared with the original molar fraction of the transition metals in precursors, the decrease of the transition metals in CuO-CoO-MnO/SiO_2 nanocomposite aerogel is probably caused by the loss of CuO, CoO, MnO and their ultrafine particles dispersed in the pores and skeletons during solvent exchange and CO_2 supercritical drying process. Moreover, the molar fractions of O and Si are 60.5% and 19.6%, respectively, and this indicates that O and Si are the dominant components in the three-dimensional structure.

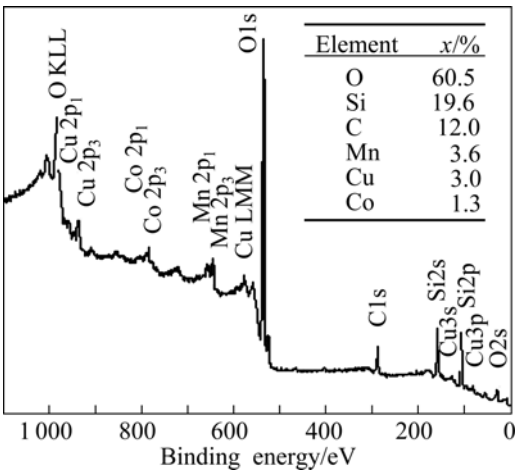

Fig.3 XPS spectra and molar fractions of atoms in CuO-CoO-MnO/SiO_2 nanocomposite aerogel heat-treated at 500 °C

Figs.4, 5 and 6 show the XPS spectra of copper, cobalt and manganese compounds in CuO-CoO-MnO/SiO_2 nanocomposite aerogel, respectively. From the main peaks in Figs.4, 5 and 6, it can be seen that the binding energy values of major copper, cobalt and manganese

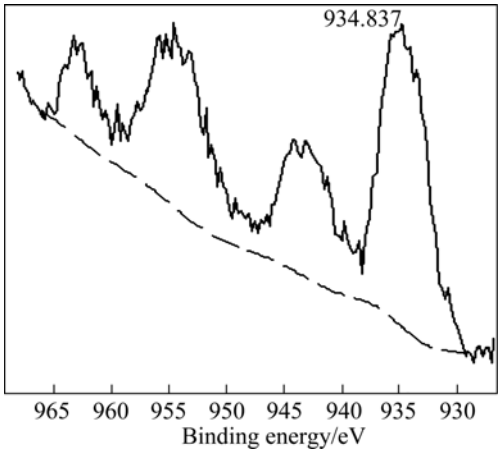

Fig.4 XPS spectra of copper compounds in CuO-CoO-MnO/SiO_2 nanocomposite aerogel heat-treated at 500 °C

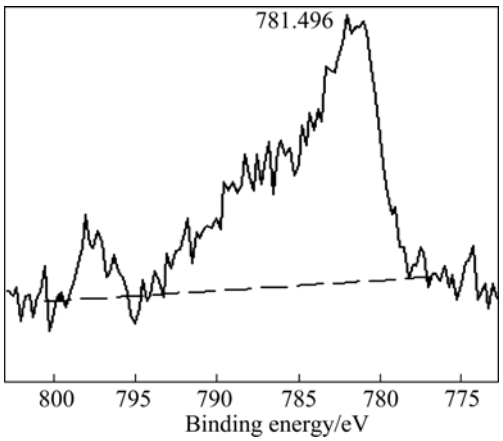

Fig.5 XPS spectra of cobalt compounds in CuO-CoO-MnO/SiO_2 nanocomposite aerogel heat-treated at 500 °C

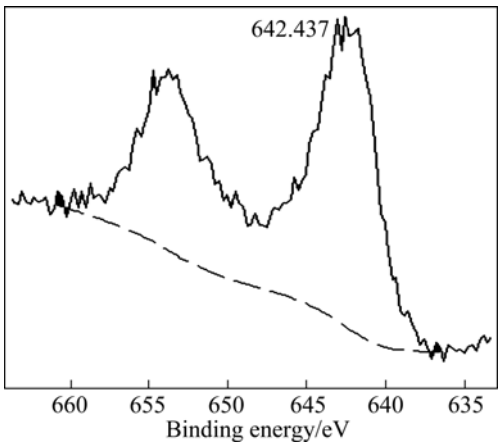

Fig.6 XPS spectra of manganese compounds in CuO-CoO-MnO/SiO_2 nanocomposite aerogel heat-treated at 500 °C

compounds are 934.837, 781.496 and 642.437 eV, respectively.

By comparing the binding energy values of Cu, Co, Mn and their oxides in Figs.4, 5 and 6 with corresponding standard binding energy values in XPS database, it can be proved that some of the transition metals exist in form of CuO, CoO, MnO and their ultrafine particles besides surface coordination bonds. Fig.7 shows the FE-SEM photograph of CuO-CoO-MnO/SiO_2 nanocomposite aerogel heat-treated at 500 °C, and the original molar fraction of transition metal oxides in precursors of the composite sol is 50%. Fig.8 shows the TEM photograph of the nanocomposite aerogel heat-treated at 500 °C. From Figs.7 and 8, we can see the ultrafine particles or aggregations of the transition metal oxides with a particle size distribution of 10−150 nm. From Fig.8, we can also see that three-dimensional network is the dominant structure in the nanocomposite aerogel. Some ultrafine particles of CuO, CoO and MnO are well-dispersed in the skeletons and pores by the separate effect of the porous network of the nanocomposite aerogel[16].

Fig.9 shows the nitrogen adsorption and desorption isotherms of CuO-CoO-MnO/SiO_2 nanocomposite aerogel without heat-treatment, and the original molar fraction of CuO, CoO and MnO in precursors of the composite sol is 50%. From Fig.9, we can see a noticeable hysteresis loop in the nitrogen adsorption and desorption isotherms. According to the classification standard of International Union of Pure and Applied Chemistry (IUPAC) on nitrogen adsorption and desorption isotherms, the isotherms in Fig.9 should belong type Ⅳ of six categories isotherms[17], which suggests the presence of mesopores with cylindrical and slit shapes in the nanocomposite aerogel[18]. Fig.10 shows the pore size distribution of the nanocomposite aerogel. From Fig.10, it can be seen that the nanocomposite aerogel is porous with a pore size distribution of 2−16 nm and an average pore size of 7.68 nm. The effect of transition metal oxides introduced into precursors on specific surface areas of CuO-CoO-MnO/SiO_2 nanocomposite aerogels is listed in Table 2. From Table 2, it can be seen that the specific surface areas of CuO-CoO-MnO/SiO_2 nanocomposite aerogels gradually decrease with the increase of transition metal oxides introduced into the precursors. Moreover, from Table 2, we can see that the specific surface area of the nanocomposite aerogel with 50% (mole fraction) transition metal oxides in the precursors and ethanol supercritical drying technique is almost twice that of the nanocomposite aerogel with the same quantity of transition metal oxides in the precursors and CO_2 supercritical drying technique. Therefore, ethanol supercritical drying technique is a better choice of drying processes because of higher specific surface area and molar fraction of transition metals in CuO-CoO-MnO/SiO_2 nanocomposite aerogels.

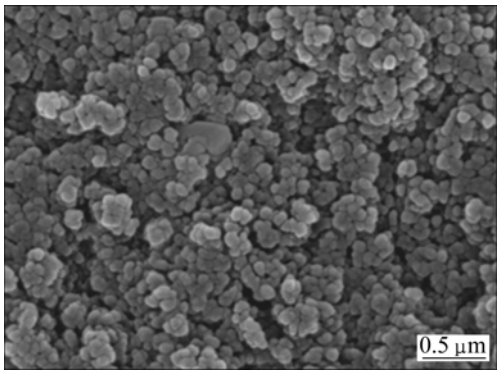

Fig.7 FE-SEM photograph of CuO-CoO-MnO/SiO_2 nanocomposite aerogel heat-treated at 500 °C

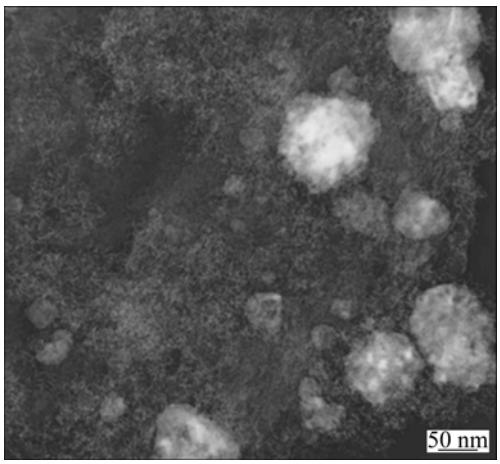

Fig.8 TEM photograph of CuO-CoO-MnO/SiO_2 nanocomposite aerogel heat-treated at 500 °C

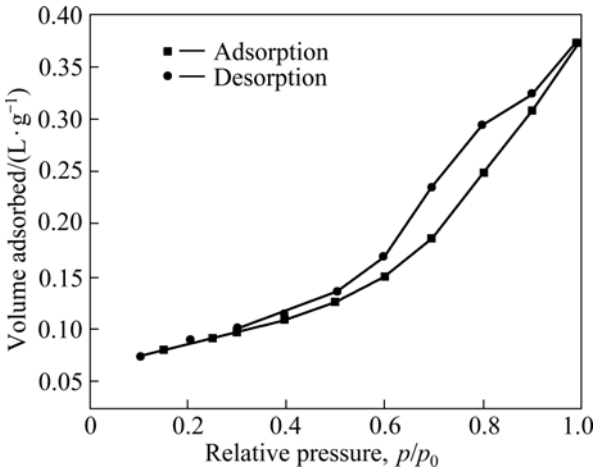

Fig.9 Nitrogen adsorption and desorption isotherms of CuO-CoO-MnO/SiO_2 nanocomposite aerogel without heat-treatment

3.3 Effect of transition metals content in precursors on composition of nanocomposite aerogels

Fig.11 shows the relationship between the mole

fraction of transition metals in CuO-CoO-MnO/SiO_2 nanocomposite aerogels and that introduced into precursors of the composite sols after solvent exchange and ethanol supercritical drying process. From Fig.11, it can be seen that the mole fraction of transition metals in the nanocomposite aerogels linearly increases with the increase of transition metals introduced into precursors.

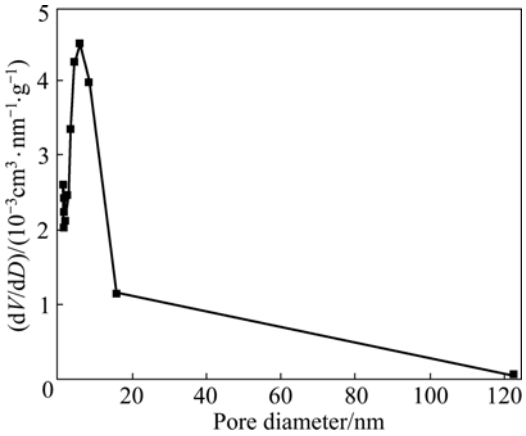

Fig.10 Pore size distribution of CuO-CoO-MnO/SiO_2 nanocomposite aerogel without heat-treatment

Table 2 Effect of transition metal oxides introduced into precursors on specific surface areas of CuO-CoO-MnO/SiO_2 nanocomposite aerogels heat-treated at 500 °C

Mole fraction of transition metal oxide/%	Supercritical drying media	Specific surface area/($m^2 \cdot g^{-1}$)
20	Ethanol	695.8
30	Ethanol	691.5
40	Ethanol	678.0
50	Ethanol	664.4
60	CO_2	384.9

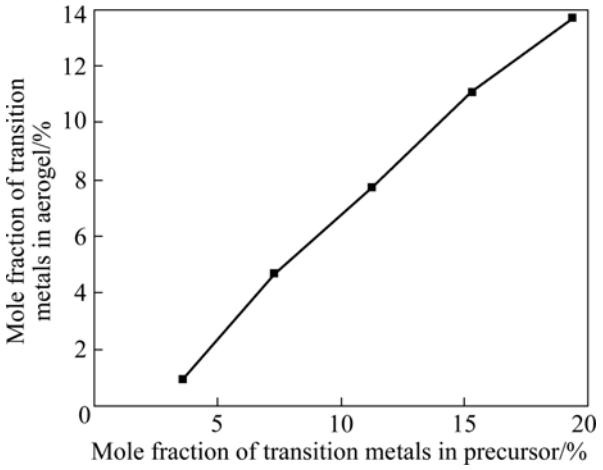

Fig.11 Relationship between mole fraction of transition metals in CuO-CoO-MnO/SiO_2 nanocomposite aerogels and that introduced into precursors

The reduction of the transition metal content should be ascribed to the loss of components during solvent exchange and supercritical drying.

4 Conclusions

1) CuO-CoO-MnO/SiO_2 nanocomposite aerogels have a three-dimensional network structure. According to the different proportions between acetates of transition metals and tetraethyl orthosilicate, bridge bonds of —O—M—O— in the network structure can be formed to some extent by the chemical bonding of transition metals and oxygen, and three-dimensional network structure is formed by the chemical bonding of Si and —O—M—O—. Some ultrafine particles of CuO, CoO and MnO are fairly well-dispersed in the skeletons and pores of CuO-CoO-MnO/SiO_2 nanocomposite aerogels by the separate effect of the porous network of aerogels.

2) CuO-CoO-MnO/SiO_2 nanocomposite aerogels are porous with a particle size distribution of 10–150 nm, a pore size distribution of 2–16 nm, an average pore size of 7.68 nm, and a specific surface area of 664.4–695.8 m^2/g. The molar fraction of transition metals in the nanocomposite aerogels is 0.71%–13.77%. This kind of structure is not only favorable to increase the loading of catalysts, but also to make full use of the effect of transition metal oxides as cocatalysts. It is a safer and environment-friendly process for diphenyl carbonate production and other fields of catalysis.

References

[1] LEVENTIS N, ELDER I A, ROLISON D R, ANDERSON M L, MERZBACHER C. Durable modification of silica aerogel monoliths with fluorescent 2, 7-diazapyrenium moieties. Sensing oxygen near the speed of open-air diffusion [J]. Journal of Chemistry Materials, 1999, 11(1): 2837−2845.

[2] MEENAKSHI G, RITSUKO N, MITSURU U. Direct synthesis of diphenyl carbonate by oxidative carbonylation of phenol using Pd-Cu based redox catalyst [J]. Journal of Molecule Catalysis, A Chem, 1999, 137(2): 147−154.

[3] XUE Wei, WANG Yan-ji, ZHAO Xin-qiang. Oxidative carbonylation of phenol over the mesoporous palladium-copper-oxide/silica catalyst prepared by sol-gel coupling with W/O microemulsion [J]. Catalysis Today, 2005, 105(3): 724−728.

[4] XUE Wei, ZHAO Xin-qiang, WANG Yan-Ji. Effect of promoter copper on the oxidative carbonylation of phenol over the ultrafine embedded catalyst Pd-Cu-O/SiO_2 [J]. Journal of Molecule Catalysis, A Chem, 2005, 232(2): 77−81.

[5] XUE Wei, ZHAO Xin-qiang, WANG Yan-ji. Oxidative carbonylation of phenol to diphenyl carbonate catalyzed by ultrafine embedded catalyst Pd–Cu–O/SiO_2 [J]. Catalysis Communications, 2005(6): 431−436.

[6] MOHANAN J L, BROCK S L. Influence of synthetic and processing parameters on the surface area, speciation, and particle formation in copper oxide/silica aerogel composites [J]. Chemistry Materials, 2003, 15(2): 2567−2576.

[7] GUO Hong-xia, CHEN Hong-ping, LIANG Ying-Hua, RUI Yu-lan,

LÜ Jing-de, FU Zhan-da. Direct synthesis of diphenyl carbonate with heterogeneous catalyst and optimal synthesis conditions of the support prepared by sol-gel method [J]. Chinese Journal of Chemical Engineering, 2008, 16(2): 223−227.

[8] CHEN Yi-min, XU Jing, XIE Kai. Preparation and characterization of Cu/SiO_2 nanocomposite aerogels [J]. Material Engineering, 2005(8): 43-46. (in Chinese)

[9] XU Jing, XIE Kai, CHEN Yi-min. Structure and catalysis of SiO_2/M nanocomposite [J]. New Chemical Material, 2002, 30(5): 32−34. (in Chinese)

[10] MA Zhi-ru, BRIAN C D, GREGOR C T. Solid state NMR investigation of silica aerogel supported Fischer–Tropsch catalysts [J]. Fuel Processing Technology, 2007, 88(2): 29−33.

[11] YOUNG S K, JARRETT W L, MAURITZ K A. Studies of the aging Nafion®/silicate nanocomposites using ^{29}Si solid state NMR spectroscopy [J]. Polym Eng Sci, 2001, 41(3): 1529−1539.

[12] ERNST B, LIBS S, CHAUMETTE P. Preparation and characterization of Fischer-Tropsch active Co/SiO_2 catalysts [J]. Applied Catalysis A: General, 1999, 186(3): 145−168.

[13] RASSY H E, PIERRE, A C. NMR and IR spectroscopy of silica aerogels with different hydrophobic characteristics [J]. Journal of Non-Crystalline Solids, 2005, 351(1): 1603−1610.

[14] ERNST B, LIBS S, CHAUMETTE P, KIENNEMANN A. Preparation and characterization of Fischer–Tropsch active Co/SiO_2 catalysts [J]. Applied Catalysis A: General, 1999, 186(3): 145−168.

[15] ZHAO Yue-qing, ZHAO Hai-lei, LIANG Ying-hua, JIA Qian-yi. Preparation and gelatination mechanism of CuO(CoO,MnO)/SiO_2 nanocomposite aerogel as catalyst carrier by sol-gel process [J]. Journal of Chinese Ceramic Society, 2008, 36(5): 658−662. (in Chinese)

[16] ZHAO Yue-qing, ZHAO Hai-lei, JIA Qian-yi, LIANG Ying-hua. Preparation and characterization of CuO(CoO, MnO)/SiO_2 nanocomposite aerogel as catalyst carrier by sol-gel process [J]. Journal of Functional Materials, 2009, 40(2): 317−321. (in Chinese)

[17] GREGG S J, SING K S W. Adsorption surface area and porosity, 2nd ed [M]. New York: Academic Press Inc, 1982: 1−287.

[18] SING K S W, EVERETT D H, HAUL R A W. Reporting physisorption data for gas/solid systems with special reference to the determination of surface area and porosity [J]. Pure Applied Chemistry, 1985, 57(2): 603−619.

(Edited by LI Xiang-qun)